

Effective non-Hermitian Hamiltonian and continuum shell model

Alexander Volya¹ and Vladimir Zelevinsky^{2,3}

¹*Physics Division, Argonne National Laboratory, Argonne, Illinois 60439**

²*National Superconducting Cyclotron Laboratory, Michigan State University, East Lansing, Michigan 48824*

³*Department of Physics and Astronomy, Michigan State University, East Lansing, Michigan 48824*

(Dated: October 23, 2018)

The intrinsic dynamics of a system with open decay channels is described by an effective non-Hermitian Hamiltonian which at the same time allows one to find the external dynamics, - reaction cross sections. We discuss ways of incorporating this approach into the shell model context. Several examples of increasing complexity, from schematic models to realistic nuclear calculations (chain of oxygen isotopes), are presented. The approach is capable of describing a multitude of phenomena in a unified way combining physics of structure and reactions. Self-consistency of calculations and threshold energy dependence of the coupling to the continuum are crucial for the description of loosely bound states.

PACS numbers: 21.60.Cs, 24.10.Cn, 24.10.-i, 42.50.Fx

I. INTRODUCTION

The center of interest in modern nuclear physics has recently moved toward nuclei far from the valley of stability. Weakly bound nuclei cannot be fully described in the limited framework of the shell model with a discrete energy spectrum. Even the properties of their bound states reflect the proximity of the continuum. Loosely bound nucleons create an extended spatial structure that determines the results of possible reactions so that nearly all excitation mechanisms break up the nucleus. The standard approaches of many-body theory, such as the Hartree-Fock-Bogoliubov mean field and random phase approximation, necessarily include virtual and real excitations to the continuum. The Borromean cases of ⁶He, ⁹Be, and ¹¹Li, when the system can be considered to be made of three clusters with all two-body subsystems being unbound, are very sensitive to the continuum physics. This is the area where the conventional division of nuclear physics into “structure” and “reactions” becomes inappropriate, and the two views of the process, from the inside (structure and properties of bound states) and from the outside (cross sections of reactions), should be recombined.

The broad success of the nuclear shell model with effective interactions urges one to look for ways to incorporate the rich experience accumulated in the shell model into a more general context which would properly include the continuum part. We will not discuss below the most complicated task in this direction, namely the problem of the effective interaction. It is virtually unknown what should be an effective interaction of quasiparticles in the restricted shell model space which includes the continuum. The work that started with the Brueckner-Bethe theory of the *G*-matrix has to be reviewed and modified.

Our goal here is much less ambitious. We would like to

demonstrate the new qualitative effects that emerge with the simple reformulation of the shell model in terms of an effective non-Hermitian and energy-dependent Hamiltonian describing the “inside” view of the dynamics in a many-body system of interacting particles coupled to and through the decay channels. For our limited purpose below we assume that the effective interaction of the shell model can be simply readjusted to the new problem, although in fact it can be non-Hermitian by itself.

The description with the aid of an effective non-Hermitian Hamiltonian is well known going back to the classical Weisskopf-Wigner damping theory [1], works in atomic physics by Rice [2] and Fano [3] and projection formalism by Feshbach [4]. The consistent formulation of the approach was given in the book by Mahaux and Weidenmüller [5] in application to processes with one particle in the continuum. This gave rise to the shell model embedded in the continuum [6, 7] recently revived [8, 9, 10] for the description of loosely bound nuclei. Another direction of development was related to the description of statistical and chaotic phenomena in nuclear reactions [11, 12] and generalization of random matrix theory [13, 14] for unstable systems. The detailed study of the effective non-Hermitian Hamiltonian revealed new collective phenomena [13, 15] with bright manifestations in nuclear physics of low [16, 17] and intermediate [18, 19] energies, atomic physics [20, 21], molecular physics [22], quantum chemistry [23], and condensed matter physics [24, 25, 26]. The basic origin of this collectivity is the same as in the Dicke superradiance [27], coherent coupling of intrinsic states through common decay channels (common radiation field of atoms confined to a small volume in the Dicke case). The ideas related to this approach were used for an analysis of experimental data, especially in two-state examples [28, 29] taken from nuclear and mesonic physics as well as from the microwave cavity experiments [30, 31, 32]. Here we follow a generic path of the shell model, adding continuum effects by including explicitly non-Hermitian terms in the Hamiltonian [33, 34].

*Electronic address: volya@anl.gov

II. NON-HERMITIAN HAMILTONIAN

We will not repeat here the full derivation of the effective non-Hermitian Hamiltonian that can be achieved by separating the full Hilbert space into the intrinsic part and the continua and eliminating the continuum part with the aid of projection operators. This procedure was addressed in detail by many authors, see for example [7, 35]. We label intrinsic states by $1, 2, \dots$, and the continuum channels by a, b, c, \dots . The matrix elements of the effective intrinsic Hamiltonian can be written as

$$\mathcal{H}_{12} = H_{12} + \Delta_{12} - \frac{i}{2}W_{12}, \quad (1)$$

where H is an internal, let us say, a standard shell-model part, and the last two terms, which in general are functions of running total energy E , are generated by the exclusion of the continuum.

The imaginary part $W(E)$ originates from the real processes of decay to channels that are open at a given energy. It is represented by the residues of the on-shell terms corresponding to the delta-functions coming from the energy conservation and causality requirement imposed on the energy denominators, $E \rightarrow E^{(+)}$. The quantity W has a factorized form,

$$W_{12} = \sum_{c:\text{open}} A_1^c A_2^{c*}, \quad (2)$$

where the decay amplitudes $A_1^c(E)$ are the matrix elements of the original total Hermitian Hamiltonian between the states $|1\rangle$ and $|c; E\rangle$ of different subspaces; the normalization coefficients are included in the definition of A_1^c . The second term of Eq. (1), $\Delta_{12}(E)$, originates from the principal value of the same expression and corresponds to the virtual off-shell processes taking place via the continuum. Therefore it includes contributions from all, open and closed, channels. For the system invariant under time reversal, one can use a real intrinsic basis, where the matrix elements H_{12}, Δ_{12} and A_1^c can be taken real.

The same effective Hamiltonian (1) determines the scattering amplitude and the reaction cross sections. The relation between the inside and outside views was studied in [5, 13, 15, 16, 17, 36]. The scattering matrix in the channel space describing the $b \rightarrow a$ process is given by

$$S^{ab} = (s^a)^{1/2} (\delta^{ab} - T^{ab}) (s^b)^{1/2}, \quad (3)$$

$$T^{ab} = \sum_{12} A_1^{a*} \left(\frac{1}{E - \mathcal{H}} \right)_{12} A_2^b. \quad (4)$$

Here $s^a = \exp(2i\delta_a)$ stands for the smooth scattering phase coming from remote resonances not accounted for explicitly. The propagator $(E - \mathcal{H})^{-1}$ in the scattering amplitude T^{ab} does not depend on a specific reaction and contains the full effective Hamiltonian (1) with the same

amplitudes A_1^c as those determining the entrance and exit channels in Eq. (4). This guarantees the unitarity of the S -matrix since the virtual processes of evolution of the open system to and from the continuum channels are included in all orders in the propagator. Indeed, if one introduces the intrinsic Hermitian propagator $(E - H)^{-1}$ and the second order Hermitian scattering amplitude,

$$K^{ab} = \sum_{12} A_1^{a*} \left(\frac{1}{E - H} \right)_{12} A_2^b, \quad (5)$$

where the propagation does not include the coupling to continuum, the full scattering amplitude is given by the geometric series (the hats mark the operators in the channel space),

$$\hat{T} = \frac{\hat{K}}{1 + (i/2)\hat{K}}. \quad (6)$$

Then the scattering matrix is explicitly unitary,

$$\hat{S} = \hat{s}^{1/2} \frac{1 - (i/2)\hat{K}}{1 + (i/2)\hat{K}} \hat{s}^{1/2}. \quad (7)$$

The diagonalization of the non-Hermitian Hamiltonian (1) produces the complex eigenvalues

$$\mathcal{E}_\alpha(E) = \tilde{E}_\alpha(E) - \frac{i}{2}\Gamma_\alpha(E), \quad (8)$$

where the real, \tilde{E}_α , and imaginary, Γ_α , parts are functions of running real energy E . Without explicit energy dependence of the effective Hamiltonian, these eigenvalues would provide the unstable states with a pure exponential decay law $\propto \exp(-\Gamma_\alpha t)$. The presence of energy dependence violates the exponential decay, and the actual quasistationary states are found at real energies E_α determined by the self-consistency condition

$$\tilde{E}_\alpha(E_\alpha) = E_\alpha. \quad (9)$$

The line-shape is not Breit-Wigner but we still call $\Gamma_\alpha(E_\alpha)$ the width of the resonance α . In what follows we omit the tilde sign for E_α if it does not lead to a confusion.

In the region of interest, namely for loosely bound systems, the main energy dependence comes from the proximity of thresholds as was stressed in Refs. [15, 33]. The channel c is open only if the total energy E is above the threshold energy $E^{(c)}$ for this channel. The decay amplitudes associated with the channel c contain therefore the step factor $\Theta(E - E^{(c)})$ and can be written as

$$A_1^c = a_1^c(E) \Theta(E - E^{(c)}), \quad (10)$$

where $a_1^c(E)$ is a smooth function of energy that falls off to zero when energy decreases to the threshold value. For a single-particle decay channel, it can be parameterized [15, 33] as proportional to the square root of the penetrability in this channel.

The real part Δ of the effective potential can be written as the principal value integral

$$\Delta_{12}(E) = \frac{\mathcal{P}}{\pi} \sum_c \int_{E(c)} \frac{dE'}{E - E'} a_1^c(E') a_2^{c*}(E'). \quad (11)$$

Under the same assumption of a non-singular character of a_1^c , the matrix elements (11) also have a smooth energy dependence with no singularities near threshold, and can be approximated by energy-independent quantities as in [15, 33].

One formal conclusion concerning the existence of bound and unbound states can be reached just from the way the theory is constructed. If the conventional shell model with a purely discrete spectrum (no coupling to the continuum) predicts a state with energy below all decay thresholds, this state will remain bound in the full calculation with the decay amplitudes included. Indeed, all widths depend on the total energy and vanish below thresholds so that the old solution is still valid. However, this statement is formal since it assumes that the reaction thresholds are known beforehand. In fact, they have to be determined consistently for the chain of nuclides relevant to the reactions under consideration.

Certainly, there are limitations in the applicability of the effective non-Hermitian Hamiltonian method in the form outlined in the present article. As energy increases, a rapid growth of a number of interfering open channels makes this approach impractical. The approximations of a different type can be then introduced in the general framework, see for example [36, 37], that directly lead to quantum kinetics of statistical reactions [38]. We also deliberately limit ourselves here by taking into account only the energy-dependence associated with threshold and resonance phenomena although the smooth “potential” scattering part could be included without significant difficulties via the entrance and exit scattering phases hidden in the factors s^a and s^b of Eq. (3). The full energy dependence was discussed, in particular, in Refs. [32, 39]. The main physical assumption made here is that the states under consideration are close to threshold and, at relatively low energy, only few open channels are really essential. The deviations resulting from violations of these conditions have been studied numerically in [24]. For the purpose of this paper, namely for the development of shell model methods intended for the description of low-lying states in the nuclear systems near the border of stability, the presumed conditions are usually fulfilled to within a sufficient accuracy.

III. SHELL MODEL APPROXIMATION

We view the Hamiltonian (1) as a sum of three terms,

$$\mathcal{H} = H^\circ + V - \frac{i}{2} W, \quad (12)$$

where we assume that the intrinsic Hermitian part $H^\circ + V$ consists of independent particle energies,

$$H^\circ = \sum \epsilon_\nu a_\nu^\dagger a_\nu, \quad (13)$$

and the effective Hermitian interaction V . As a renormalization of the standard shell model interaction, the Hermitian matrix elements Δ_{12} , Eq. (11), generated by the virtual coupling through continuum, can be incorporated into the operator V . The approximation of energy independence of the operator Δ and, as a result, energy independence of V , also used in previous works [15, 33], can be easily removed.

In order to formulate physical problems in the spirit close to the conventional shell model, we start from the basis states $|\Phi\rangle$, the eigenstates of H° , that are Slater determinants of the m -scheme or their linear combinations projected onto correct values of total spin J and isospin T . For the next step we consider the “unperturbed” part of the Hamiltonian which includes the independent particle part H° and the imaginary part $-(i/2)W$

$$\mathcal{H}^\circ = H^\circ - \frac{i}{2} W. \quad (14)$$

The diagonalization of the Hamiltonian (14) along with the self-consistent solution of Eq. (9) gives new eigenvectors $|\tilde{\Phi}\rangle$ either with complex energies (8) or as stable configurations on the real energy axis. The factorized nature of the operator W , Eq. (2), that is preserved by orthogonal transformations, and the presence of symmetries may bring additional simplifications. In some special cases, \mathcal{H}° remains diagonal in the original basis $|\Phi\rangle$. In these situations the meaning of the amplitudes is the most clear, being related to the single-particle decay into continuum.

Thus, for an isolated single-particle level $|\nu\rangle$ embedded in the continuum, the unperturbed real energy is $E_{\text{core}} + \epsilon_\nu$. If the only open channel, $c \Rightarrow \nu$, is associated with the emission of the particle ν , the imaginary part W leads to the width

$$\gamma_\nu = |A_\nu^\nu|^2 \quad (15)$$

for any configuration which consists of the particle on the level $|\nu\rangle$ and an arbitrary state of the stable core (no interaction between them at this stage). Threshold energy is determined by the core configuration. Similarly, in the case of several single-particle levels ν embedded in the continuum, the single-particle decay channels, opened for a specific configuration $|\Phi\rangle$ with occupation numbers $n_\nu(\Phi) = 0$ or 1, result in the width

$$\gamma(\Phi) = \sum_\nu n_\nu(\Phi) \gamma_\nu. \quad (16)$$

If there are several single-particle levels $|\nu_i\rangle$ with the same exact quantum numbers $j^\pi\tau$, the situation is more complicated and in general H° and \mathcal{H}° cannot be simultaneously diagonalized. Apart from the particle emission

from a given single-particle state we have now also the interaction through continuum given by the off-diagonal elements of W_{12} . Here the Dicke collectivization and redistribution of the widths [7, 13, 15] are possible, see below, and already at this stage, with no residual shell-model interaction V , we need to diagonalize the non-Hermitian Hamiltonian \mathcal{H}° .

This situation is almost certainly present in cases where two-particle emission is possible from different initial configurations. For example, a zero spin pair can be emitted from a few j -levels leading to a final state with the same quantum numbers and therefore into the same decay channel. Here the coupling through the continuum may be very important.

In the most general case, because of the energy dependence in the amplitudes A_i^\ddagger , the positions of the resulting quasistationary eigenstates of \mathcal{H}° in the complex plane should be determined avoiding false solutions that can appear due to the possible non-analytic energy dependence at thresholds. One can take only those complex poles that can be traced back to the real axis (independent particle states $|\Phi\rangle$) in the case of the closed channels. Another new feature is that, generally speaking, the threshold energies are not known *a-priori*. They are to be calculated self-consistently comparing total energies of the parent and daughter nuclei taken in the same approximation. But this must be done only on the next step when the residual shell-model interaction is accounted for.

Finally, we include an effective interaction V that introduces the mixing of (in general unstable) shell model configurations $|\tilde{\Phi}\rangle$. As a result, instead of original independent particle states, we obtain the states $|\Psi\rangle$ which characterize both the intrinsic structure and possible decay channels in the fully interacting system. Since the Hamiltonian is non-Hermitian, the resonance “energies” (8) move in the complex plane relative to their initial positions given by eigenvalues of \mathcal{H}° (states $|\tilde{\Phi}\rangle$) and this dynamics may be quite complicated driving some states back to stability.

Another important “intermediate” Hamiltonian $H^\circ + V$ describes the case when all decay widths are “switched off” and obviously corresponds to the standard shell model. Below we denote shell-model many-body eigenstates as $|\Psi_{\text{s.m.}}\rangle$. Of course, in practice it is not necessary to make a two-step diagonalization, and the intermediate steps with the wave functions $|\tilde{\Phi}\rangle$ or $|\Psi_{\text{s.m.}}\rangle$ can be avoided.

It is known, see for instance [40], that the eigenstates of a non-Hermitian Hamiltonian form a biorthogonal system which would allow one to study the observable characteristics of unstable states along with the reaction cross sections and dynamics transformed to the time domain. Below we show several examples ordered by increase of complexity, from very schematic to more realistic. The selected cases illustrate the diversity of the physical phenomena that can appear in unstable many-body systems and can be described by the method of an effective non-

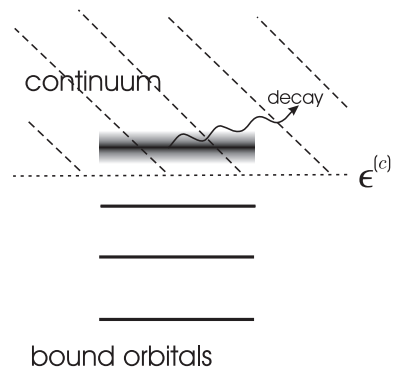


FIG. 1:

Hermitian Hamiltonian. As mentioned in the Introduction, in this exploratory study we assume the effective interaction to be known and its matrix elements V_{12} (taken in a basis of stable states and including Δ_{12}) to be real.

IV. SINGLE-PARTICLE DECAY IN A MANY-BODY SYSTEM

A. One single-particle level in the continuum; energy-independent continuum width

We start with the simplest problem (a similar example was shown in Ref. [34]). Consider a set of single-particle energies ϵ_ν with the upper of them lying above the particle emission threshold $\epsilon^{(c)}$, see Fig. 1, where a system of Ω single-particle levels is presented with $\epsilon_\nu < \epsilon^{(c)}$ for $\nu = 1, \dots, \Omega - 1$ and $\epsilon_\nu > \epsilon^{(c)}$ for $\nu = \Omega$. For simplicity we assume here that the levels are equidistant on the real axis and not degenerate; later we add the Kramers double degeneracy. We assume that all single-particle emission channels have different quantum numbers and cannot be coupled through continuum. Thus, we have only one initial non-zero single-particle width expressed with the aid of the complex single-particle energy

$$e_\nu = \epsilon_\nu - \frac{i}{2}\gamma\delta_{\nu\Omega}. \quad (17)$$

Now we use this set of single-particle levels as the basis for forming the many-body configurations $|\Phi\rangle$ as Slater determinants with all possible distributions of the occupancies n_ν . Finally we switch on a real two-body interaction V .

In order to characterize the generic results which are insensitive to specific peculiarities of the residual interaction, in this example we use a system of $N = 4$ fermions with the equidistant spectrum ϵ_ν of $\Omega = 8$ orbitals and random (Gaussian distributed) matrix elements of the two-body interaction. We solve this problem by diagonalizing the complex matrix of the full many-body Hamiltonian \mathcal{H} . The results are shown in Fig. 2 as the dynamics of the complex eigenvalues evolving as a function of

the only variable parameter, the single-particle width γ , taken here as an energy-independent number.

At $\gamma = 0$ (a normal shell-model limit), the many-body states $|\Psi_{\text{s.m.}}\rangle$ obtained with the real residual interaction are stable, and their spectrum can be represented by the points on the real axis. As γ increases, all states $|\Psi_{\text{s.m.}}\rangle \Rightarrow |\Psi\rangle$ acquire widths and move into the complex plane. This means that, because of the unrestricted configuration mixing, any many-body eigenstate $|\Psi\rangle$ contains an admixture of configurations with the occupied upper orbital, and therefore it is capable of decay. In the limit of small γ , in agreement with usual perturbation theory it is expected that $|\Psi\rangle \approx |\Psi_{\text{s.m.}}\rangle$. Thus, the decay width of a many-body state Ψ is, similarly to the case of Eq. (16), determined by the spectroscopic factor of a progenitor stable state $|\Psi_{\text{s.m.}}\rangle$ that is given as an occupation probability of a decaying single-particle orbital ν ,

$$\Gamma(\Psi) = \gamma n_\nu(\Psi_{\text{s.m.}}). \quad (18)$$

This natural picture breaks down once the value of γ becomes comparable to the level spacing D along the real axis, and the internal dynamics gets affected by the continuum in a non-perturbative way.

In this example γ , and therefore the effective Hamiltonian \mathcal{H} , is independent of running energy E . This makes the trace of \mathcal{H} a conserved quantity resulting in

$$-2\text{Im}(\text{Tr } \mathcal{H}) = \sum_{\Psi} \Gamma(\Psi) = \frac{(\Omega - 1)!}{(\Omega - N)!(N - 1)!} \gamma. \quad (19)$$

The real part of the trace $\sum_{\Psi} \tilde{E}(\Psi)$ also remains constant and is independent of γ . In Eq. (19) we counted the number of non-interacting configurations available for $(N - 1)$ particles if the decaying orbital is occupied. Conservation of the trace of \mathcal{H}^2 and the fact that the imaginary part W is diagonal make $(\gamma)^{-1} \sum_{\Psi} \tilde{E}(\Psi)\Gamma(\Psi)$ also a γ -independent constant.

In the $\gamma \rightarrow 0$ limit, the occupancy of the decaying orbital governs the distribution of widths in Eq. (19). This can be generalized by introducing the dynamic occupation numbers

$$n_\Omega(\Psi; \gamma) = \frac{\partial \Gamma(\Psi; \gamma)}{\partial \gamma}. \quad (20)$$

These parameters describe how at a given γ an infinitesimal increase of the initial single-particle width γ is distributed among the many-body states Ψ . According to Eq. (19), $\sum_{\Psi} n_\Omega(\Psi; \gamma)$ is independent of γ . Despite all the resemblance to occupation numbers the numbers (20) can be negative. One can also introduce generalized spectroscopic factors $\Gamma(\Psi; \gamma)/\gamma$ that are always positive and bound between 0 and 1, but being cumulative quantities they would be less sensitive to dynamical features.

With further increase of γ the picture in Fig. 2 looks paradoxical [34]. The many-body states are clearly divided into two groups. The complex energies of the first

group rapidly move away from the real axis revealing large widths. At the same time the states of the second group turn back to the real axis and keep only tiny widths, whence becoming long-lived. Similar phenomena are known for a long time from various schematic studies [41, 42] and versions of the shell model with the continuum effects included, for example [43, 44].

The puzzle is readily resolved since with γ increasing we come to the situation where the imaginary term dominates the dynamics and therefore classifies the eigenstates by their relation to decay rather than by real energy. Any superposition of configurations with a considerable amplitude of the occupied unstable level 8 undergoes fast decay. Such states constitute the first group. The superpositions of the configurations with the empty level 8 become eigenstates of the second group and correspond to long-lived compound states. It is easy to calculate the dimensions of the two groups. The total number of states \mathcal{N} for 4 fermions on 8 non-degenerate orbitals is $8!/(4!)^2 = 70$. The first group contains the states where the level 8 is occupied and the remaining 3 particles are distributed over 7 stable levels; the corresponding dimension is $7!/(3!4!) = 35$, so that the eigenstates are divided in this case evenly between the two groups, in agreement with Fig. 2.

We see that the strong coupling of intrinsic states to the continuum produces a natural segregation [13] of processes into fast direct reactions and slow compound nucleus reactions. Here the direct processes are of single-particle nature, and at large γ the corresponding width of each state of the first group is close to γ . Fig. 3, where the segregation of the effective occupation numbers is shown as a function of γ , confirms the division of states into short-lived with a fully occupied decaying single-particle orbital, $n_8 = 1$, and compound ones where $n_8 = 0$. The analog of this segregation effect has been experimentally seen [31] in microwave cavities, although for realistic systems the situation is more complicated, mainly because of the uncertainty in the effective number of open channels [26, 39].

In order to further quantify this phase transition we introduce a parameter ξ which roughly shows the fraction of segregated states lying in a small vicinity σ near $n_8 = 0$ and $n_8 = 1$,

$$\xi(\gamma) = \frac{1}{\mathcal{N}} \sum_{\Psi} \left[e^{-n_\Omega^2(\Psi)/(2\sigma^2)} + e^{-[1-n_\Omega^2(\Psi)]^2/(2\sigma^2)} \right]. \quad (21)$$

We select here $\sigma = 0.1$. In Fig. 4 the quantity ξ is plotted as a function of γ for various relative strengths of residual mixing, panel (a), and for different half-occupied systems, panel (b). It follows from the graphs of Fig. 3 and 4 that the segregation starts at $\gamma \sim D$, and occurs gradually as γ dominates the residual mixing V , resulting in a peculiar phase transition. The theory of this general phenomenon seen earlier in numerical simulations [43, 44] was developed in [13] where an analogy to the Dicke coherent state in optics [27] was pointed out. A similar

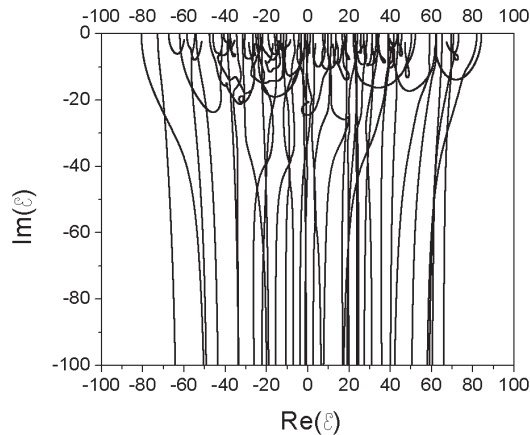


FIG. 2: Trajectories of 70 many-body states of the system of 4 particles on 8 single-particle levels are shown in a complex plane as a function of the increasing decay width γ of the upper single-particle state. The residual two-body interaction matrix elements are selected randomly from the Gaussian distribution with zero mean and with the variance of one energy unit. The single-particle energies are equidistant with a spacing $\Delta\epsilon = 0.5$ energy units.

effect, with possible implications for quantum computers, is known in the context of quantum measurement theory, where coupling and decay created by the measurement mechanism can result in a separation of dynamics into decoupled subspaces [45].

Formally the phase transition follows from the factorized structure of the continuum coupling in Eq. (2). The rank r of the matrix W is equal to the number of open channels (the dimension of the first group of states in the example of Fig. 2) that is smaller than the total dimension \mathcal{N} of the intrinsic space. This matrix has r nonzero eigenvalues whereas the remaining $\mathcal{N} - r$ eigenvalues are equal to zero. In a more specific language [13, 15], the independent particle basis $|\tilde{\Phi}\rangle$ of this example is the “doorway” basis for the coupling to and through the continuum. In the limit of strong continuum coupling, the part W dominates the dynamics and aligns the eigenstates along its eigenvectors. Similarly to the coupling of two-level atoms through their common radiation field in the Dicke superradiance, here the intrinsic states are coupled through the decay channels. At values of γ exceeding the level spacing (the regime of overlapping resonances), this coupling becomes strong, and the continuum accomplishes the self-organization of intrinsic structure [7]. The real part V of the interaction is needed only to establish the correct level density on the real axis. The random character of V in the above example does not prevent the system from the ordering by the continuum.

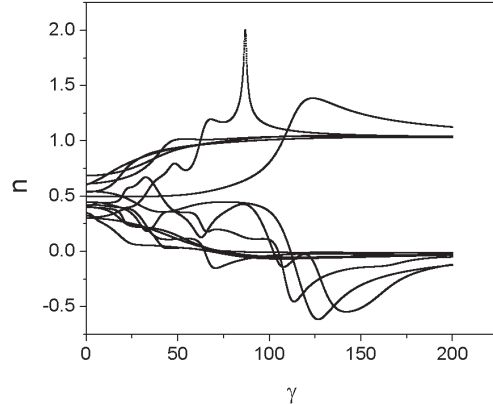


FIG. 3: The evolution of the effective occupation number n_s , Eq. (21), as a function of γ for the 13 lowest (selected at $\gamma = 0$) many-body states.

B. Two unstable single-particle levels

A slightly more complex example is shown in Fig. 5. Here we again have eight equidistant non-degenerate single-particle orbitals ϵ_ν . Two of them, with different quantum numbers, have nonzero widths equal to γ and $\gamma/2$. With the random interaction turned on, the evolution of the 70 eigenvalues with increasing γ separates four groups of the eigenstates with different decay rates, fast, slow and two intermediate. Short-lived states, type (a) in Fig. 5, include configurations with both unstable orbitals being occupied, thus at large γ their width is roughly $\Gamma^{(a)} \approx 3\gamma/2$. The number of such configurations, $6!/(2!4!) = 15$, is equal to the number of long-lived states [type (d)]. The corresponding quasi-stable configurations with $\Gamma^{(d)} \approx 0$ at $\gamma \rightarrow \infty$ do not have a noticeable admixture of unstable orbitals so that all four particles are distributed over six stable orbitals. Finally, the intermediate lifetimes $\Gamma^{(b)} \approx \gamma$ and $\Gamma^{(c)} \approx \gamma/2$ correspond to cases where only one of the unstable orbitals is filled. The number of such cases is $6!/(3!)^2 = 20$.

C. Kramers degeneracy

The manifestations of symmetries and symmetry breaking in open systems are particularly interesting and important for the shell model formalism. In the presence of global symmetry, such as rotational invariance, the entire space that includes both internal and external states, is symmetric. In this case degeneracies of states are possible and there is no mixing between the classes of states with different exact quantum numbers. A non-trivial situation occurs when symmetry is violated in external space or in the internal-external coupling, while the intrinsic system is still symmetric. Then the degen-

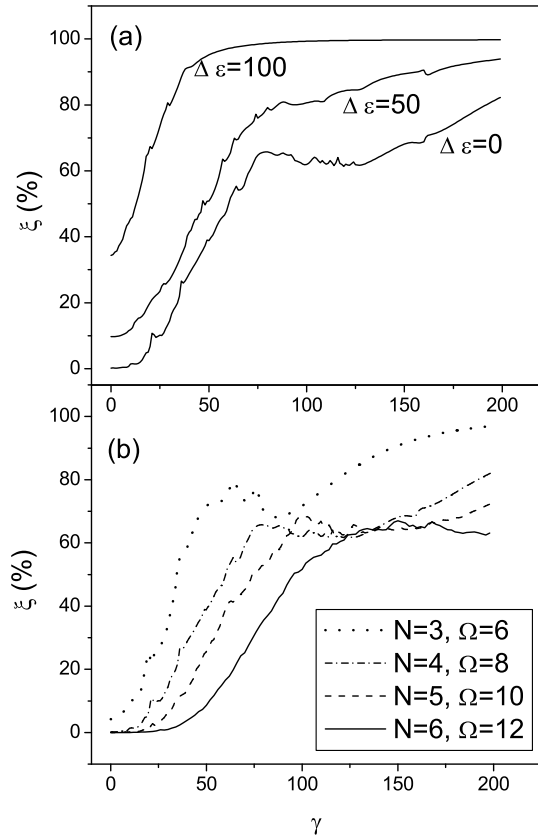


FIG. 4: Fraction of segregated states as a function of γ for the same system as in Figs. 3 and 4. For the upper panel (a) the single-particle level spacing is varied from the degenerate case, $\Delta\epsilon = 0$, to $\Delta\epsilon = 100$, a point where the residual interaction V can be completely ignored. The lower panel (b) shows the “condensed” fraction of many-body states for a degenerate single-particle spectrum and various system sizes. In all cases only one single-particle level undergoes decay with the width γ .

eracy is lifted and in the effective Hamiltonian, in general, both non-Hermitian part W and Hermitian part Δ are no longer invariant. Here we consider a schematic case when symmetry is violated only in the internal-external coupling.

In systems invariant under time reversal, the states of an odd number of fermions are at least double degenerate (Kramers degeneracy). Let our eight single-particle orbitals form four double-degenerate pairs, as it happens in the body-fixed frame of a nucleus with static multipole deformation where the degeneracy in an axially-symmetric case is connected with the sign of the magnetic quantum number, $\pm m$. This situation is shown in Fig. 6(a) for the case of 3 particles and random selection of time-reversal invariant two-body residual interaction. All curves in this figure correspond to the evolution of

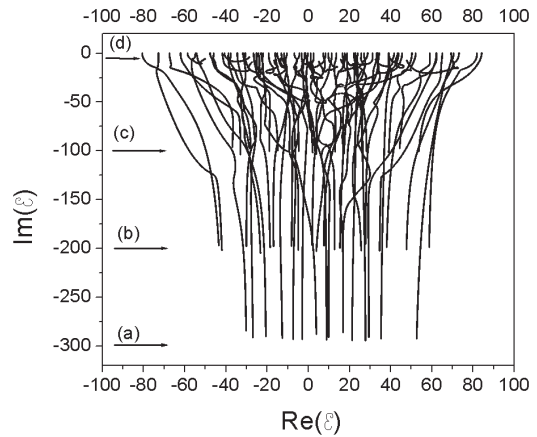


FIG. 5: Trajectories of 70 many-body states of the system of 4 particles on 8 single-particle levels are shown in a complex plane as a function of the increasing decay width, γ and $\gamma/2$, of the two upper single-particle states. The single-particle energies and the two-body interaction matrix elements are the same as in Fig. 2. Arrows (a), (b) and (c) indicate the end-points at large γ for the corresponding types of states: short-lived (a), and two intermediate types (b) and (c), see text. The remaining states of the fourth class (d) are quasistable.

double-degenerate many-body states, since two decaying Kramers-degenerate single-particle levels are assumed to have the same width, and thus the symmetry is not violated by decay.

The case (b) illustrates the situation when time-reversal invariance is slightly distorted in the decay channel, for instance by an external magnetic field, so that one of the Kramers-degenerate levels has a 10% larger width. The long-lived and short-lived states are the least affected ones, in Fig. 6(b) the splitting of their degeneracy is hard to resolve. Indeed, for both of these cases the decay dynamics either lock a particle pair on the decaying time-conjugate orbitals or make them both unoccupied. This restriction of motion allows the system to retain the quasi-invariance. The remaining states with the intermediate lifetime involve superpositions with one particle being on either of the two decaying single-particle states. Such a superposition, generally, is no longer time-reversal invariant and the Kramers degeneracy is broken. Finally, in the limit of strong decay, residual two-body interactions become less effective in mixing and then real parts of complex energies \mathcal{E} regain the degeneracy. These arguments, however, no longer hold true in the extreme limit of the violated time-reversal invariance when one of the time-conjugate orbitals becomes stable while the partner decays, Fig. 6(c). Then the Kramers degeneracy is broken and, since there is no intermediate groups, the states join long-lived or short-lived families, which leads to $35(\text{long})+21(\text{short})=56$ states.

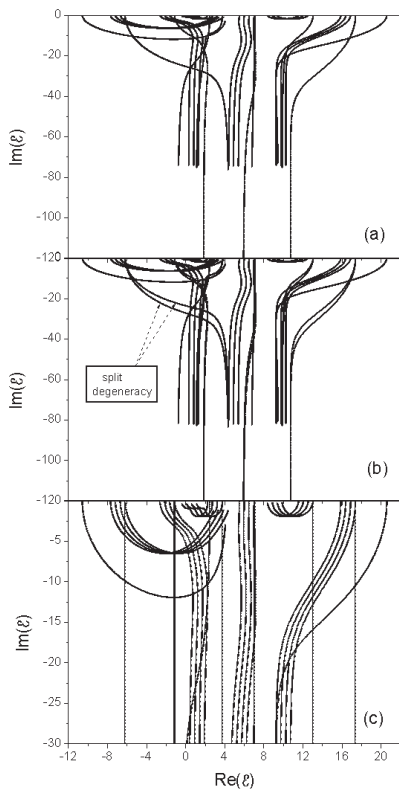


FIG. 6: Dynamics of many-body eigenstates of the system containing 4 double-degenerate single-particle states and $N = 3$ particles. Panel (a) corresponds to the upper two degenerate single-particle levels having the same width γ . The Kramers degeneracy is preserved in this case. Panels (b) and (c) correspond to the situations where the invariance is broken by the decay. In (b) the upper pair of initially degenerate time-conjugate levels have widths γ and 1.1γ , respectively. The case (c) presents the maximum symmetry violation as the time-conjugated levels have widths γ and 0.

V. DYNAMICS OF TWO STATES COUPLED TO A COMMON DECAY CHANNEL

A. Appearing of binding

Here we consider a model that shows how the attractive real interaction works generating the binding of orig-

inally unstable states in the presence of the coupling through continuum. We consider two single-particle levels, let say $s_{1/2}$ and $p_{1/2}$ orbitals, in the continuum so that their energies $\epsilon(s)$ and $\epsilon(p)$ are positive if the continuum threshold is put at zero energy. In the three-body Borromean model for ^{11}Li with the inert core of ^9Li and particle-unstable ^{10}Li , the two active states are those for a pair of halo neutrons, $\epsilon_1 = 2\epsilon(p)$, $\epsilon_2 = 2\epsilon(s)$. They are quasistationary, and their decay amplitudes $A_{1,2}$ for the only open channel, characterized by the core nucleus in the ground state and the neutron pair in the state $J^\pi = 0^+$ in the continuum, can be found from a single-particle picture. At this point the exact form of the energy dependence is not fixed, except for the fact that when the total energy approaches zero, the decay becomes forbidden so that, as in Eq. (10), the amplitudes $A_{1,2}$ contain the step function $\Theta(E)$. A special case with one initial non-zero width was presented in [33]. The problem of two-body decay, especially relevant for Borromean systems, was recently approached with the use of different shell model formalisms in Refs. [9, 10]. Two-proton radioactivity [46] is another example requiring a similar consideration.

According to Sect. II, the effective non-Hermitian Hamiltonian in this 2×2 space is

$$\mathcal{H} = \begin{pmatrix} \epsilon_1 - \frac{i}{2}\gamma_1 & v - \frac{i}{2}A_1A_2 \\ v - \frac{i}{2}A_1A_2 & \epsilon_2 - \frac{i}{2}\gamma_2 \end{pmatrix}. \quad (22)$$

Here $V_{12} \equiv v$ is the real mixing matrix element, $\gamma_{1,2} = A_{1,2}^2$, and the amplitudes $A_{1,2}$ are also real. One should be careful with the phases. For a pure internal interaction, the sign of the mixing matrix element V_{12} is irrelevant, it always can be changed by the redefinition of the phase of one of the states, 1 or 2. But with coupling to continuum this change must be accompanied by the corresponding phase change in the decay amplitude; therefore we cannot simply put $A_{1,2} = \sqrt{\gamma_{1,2}}$.

Formal diagonalization of the effective Hamiltonian gives the complex energies of the quasistationary states

$$\mathcal{E}_\pm = \frac{1}{2} \left[\epsilon_1 + \epsilon_2 - \frac{i}{2}(\gamma_1 + \gamma_2) \right] \pm \frac{1}{2} \left\{ (\epsilon_1 - \epsilon_2)^2 + 4v^2 - \frac{1}{4}(\gamma_1 + \gamma_2)^2 - i[(\epsilon_1 - \epsilon_2)(\gamma_1 - \gamma_2) + 4vA_1A_2] \right\}^{1/2}. \quad (23)$$

Let us check some particular cases.

(i) For the case of stable states, $A_{1,2} = 0$, we come to

the standard two-level repulsion,

$$\mathcal{E}_\pm = E_\pm = \frac{1}{2} \left[\epsilon_1 + \epsilon_2 \pm \sqrt{(\epsilon_1 - \epsilon_2)^2 + 4v^2} \right]. \quad (24)$$

The lower level reaches zero energy under the condition

$$v^2 = \epsilon_1 \epsilon_2. \quad (25)$$

(ii) Consider the case with no intrinsic mixing, $v = 0$, and two degenerate resonances, $\epsilon_1 = \epsilon_2 \equiv \epsilon$. Then the Hamiltonian consists of the unit matrix ϵ and the matrix W of a special factorized type (rank $r = 1$) so that the correct linear combinations are the eigenvectors of W ; one of them, the analog of the Dicke coherent state, should accumulate the total width, and the second should be stable. Indeed, Eq. (23) gives in this case

$$\begin{aligned} \mathcal{E}_\pm &= \epsilon - \frac{i}{4}(\gamma_1 + \gamma_2) \pm \frac{i}{4}(\gamma_1 + \gamma_2) \\ \Rightarrow \begin{cases} E = \epsilon, & \Gamma = 0, \\ E = \epsilon - \frac{i}{2}\Gamma, & \Gamma = \gamma_1 + \gamma_2 \end{cases} \end{aligned} \quad (26)$$

One of such situations with a bound state in the continuum was discussed in [47] and explained in terms of the effective Hamiltonian in [15].

(iii) In contrast to the avoided crossing (24) of stable levels, the coincidence of two complex eigenvalues is possible. It requires that two conditions be fulfilled,

$$(\epsilon_1 - \epsilon_2)^2 = \gamma_1 \gamma_2, \quad (27)$$

and

$$(\gamma_1 - \gamma_2)^2 = 16v^2. \quad (28)$$

The coinciding complex energies \mathcal{E}_\pm , Eq. (23), evenly divide the trace of the Hamiltonian. In the energy-independent two-level Hamiltonian [48] the condition for crossing is

$$(\epsilon_1 - \epsilon_2)(\gamma_1 - \gamma_2) + 4vA_1A_2 = 0. \quad (29)$$

Which leads to crossing of either real energies $E_+ = E_-$ or widths $\Gamma_+ = \Gamma_-$ depending if the sign of

$$X = (\epsilon_1 - \epsilon_2)^2 + 4v^2 - \frac{1}{4}(\gamma_1 + \gamma_2)^2 \quad (30)$$

is negative or positive, respectively. Clearly, in the energy-dependent case same remain true for the crossing of energies, other conditions, such as for crossing of the widths change because generally $\mathcal{H}(E_+) \neq \mathcal{H}(E_-)$. The crossing and anti-crossing of unstable levels were theoretically discussed also in Ref. [21, 35] and experimentally studied with microwave cavities [30].

The secular equation for the eigenvalues can be also written in a form explicitly separating the real, \tilde{E} , and imaginary, $\tilde{\Gamma}$, parts of complex roots (here we again restore the tilde sign in order to distinguish the roots from the running energy value E). The real part of this equation gives

$$\tilde{E}^2 - \tilde{E}(\epsilon_1 + \epsilon_2) - \frac{\tilde{\Gamma}}{4}(\tilde{\Gamma} - \gamma_1 - \gamma_2) + \epsilon_1 \epsilon_2 - v^2 = 0, \quad (31a)$$

while from the imaginary part we obtain

$$\tilde{\Gamma} = \frac{\tilde{E}(\gamma_1 + \gamma_2) - \gamma_1 \epsilon_2 - \gamma_2 \epsilon_1 + 2vA_1A_2}{2\tilde{E} - \epsilon_1 - \epsilon_2}. \quad (31b)$$

The coupled Eqs. (31a) and (31b) determine \tilde{E} and $\tilde{\Gamma}$. For an arbitrary energy dependence of the amplitudes $A_{1,2}(E)$ that, in order to find the quasistationary states, are to be taken in these equations at $E = \tilde{E}$, this is still an implicit solution; even the number of roots can change.

For a sufficiently strong interaction v , the repulsion of real energies can bring the lower eigenvalue E_- to zero (a threshold value). Then both amplitudes $A_{1,2}$ disappear together with the eigenwidth Γ_- , Eq. (31b). This means that the lowest quasistationary state becomes bound under the same condition (25). If the mixing increases further, the binding energy of the lower state is going down,

$$E_- \approx -\frac{v^2 - \epsilon_1 \epsilon_2}{\epsilon_1 + \epsilon_2}. \quad (32)$$

As was mentioned in [33] for a similar model with only one non-vanishing γ , this is a prototype of the dynamics leading to the binding of nuclei as ^{11}Li where the residual interaction among the valence neutrons is, as we have assumed in this Section, of pairing type.

The higher level, in the point of bifurcation (25), has the energy

$$E_+ = \frac{1}{2} \left[\epsilon_1 + \epsilon_2 + \sqrt{(\epsilon_1 + \epsilon_2)^2 + \Gamma_+(\Gamma_+ - \gamma_1 - \gamma_2)} \right], \quad (33)$$

where $\gamma_{1,2}$ are to be taken at energy $E = E_+$. If the effective Hamiltonian were energy-independent, both the real and imaginary parts of its trace would be separately preserved by the complex orthogonal transformation to the eigenvectors. This means that we would always have

$$\Gamma_+ + \Gamma_- = \text{tr } W = \gamma_1 + \gamma_2 \quad (34)$$

and

$$E_+ + E_- = \text{tr } \epsilon = \epsilon_1 + \epsilon_2. \quad (35)$$

At the bifurcation point, $E_- = \Gamma_- = 0$, we would have

$$\Gamma_+ = \gamma_1 + \gamma_2, \quad E_+ = \epsilon_1 + \epsilon_2, \quad (36)$$

while it follows from Eqs. (25) and (31b) that

$$\Gamma_+(E_+) = \frac{[A_1(E_+)\sqrt{\epsilon_1} + A_2(E_+)\sqrt{\epsilon_2}]^2}{\epsilon_1 + \epsilon_2} \quad (37)$$

and

$$\begin{aligned} &\Gamma_+(E_+) - \gamma_1(E_+) - \gamma_2(E_+) \\ &= -\frac{[A_1(E_+)\sqrt{\epsilon_2} - A_2(E_+)\sqrt{\epsilon_1}]^2}{\epsilon_1 + \epsilon_2} < 0, \end{aligned} \quad (38)$$

in contradiction to the first part of Eq. (36). The trace violation occurs because the imaginary parts have their own energy behavior with compulsory zero-energy thresholds. When the levels are repelled by the mixing interaction, their widths are changed by the dynamics outside the 2×2 matrix. But the trace is preserved and Eq. (36) is fulfilled if

$$\frac{A_1(E)}{A_2(E)} = \sqrt{\frac{\epsilon_1}{\epsilon_2}}, \quad (39)$$

so that in the entire energy range of interest the two partial widths grow proportionally, an interesting exceptional case.

B. Scattering cross section

In this subsection we consider the scattering cross section for the case of two intrinsic states coupled to one open channel. Although this cannot be observed with the scattering of a neutron pair, the result is relevant for the excitation processes of a Borromean system. The elastic cross section in the s -wave for a relative momentum $k \propto \sqrt{E}$ is

$$\sigma(E) = \frac{\pi}{k^2} |S(E) - 1|^2, \quad (40)$$

where the scattering matrix is defined by Eqs. (4) and (8) in terms of the effective Hamiltonian \mathcal{H} . In our case, Eq. (22), neglecting the potential scattering s , the propagator can be easily found, and we obtain

$$T(E) = \frac{E(\gamma_1 + \gamma_2) - \gamma_1\epsilon_2 - \gamma_2\epsilon_1 - 2vA_1A_2}{(E - \mathcal{E}_+)(E - \mathcal{E}_-)}, \quad (41)$$

with the poles $\mathcal{E}_\pm = E_\pm - (i/2)\Gamma_\pm$ given by Eq. (23), or by a pair of coupled equations (31). One can notice that the relative sign of the matrix elements for the direct internal interaction between the mixed states, v , and for their continuum mediated interaction, A_1A_2 , may considerably change the resulting cross section.

In the special case [(ii), Sect. VA] of a pair of degenerate intrinsic levels with no direct interaction, Eq. (26), the general result (41) reduces formally to the single Breit-Wigner resonance on a Dicke coherent state,

$$T(E) = \frac{\gamma_1 + \gamma_2}{E - \epsilon + (i/2)(\gamma_1 + \gamma_2)}. \quad (42)$$

The second root, $\Gamma = 0$, of Eq. (26) is decoupled from the continuum and does not influence the scattering process. We have to stress again that the “widths” $\gamma_{1,2}$ in general depend on running energy E .

At the bifurcation point (25), the scattering amplitude becomes

$$T(E) = \frac{E(\gamma_1 + \gamma_2) - (A_1\sqrt{\epsilon_2} + A_2\sqrt{\epsilon_1})^2}{E(E - \mathcal{E}_+)}, \quad (43)$$

where the higher root \mathcal{E}_+ is defined by Eqs. (33) and (37). At low energy, $E \rightarrow 0$, the behavior of the scattering cross section, as well as photonuclear processes, is determined by the actual energy dependence of decay amplitudes.

C. Solutions with energy-dependent widths

In this and the next subsections we illustrate the discussed above dynamics of two states coupled to a common continuum. For all figures here we assume that $\epsilon_1 = 100$ keV and $\epsilon_2 = 200$ keV for the particle pair in p and s states, respectively. For these parameters the ground state reaches zero energy, and thus becomes bound, at $v \approx 141$ keV by virtue of Eq. (25).

The picture with energy-independent widths is not consistent with the definition of thresholds. As seen from Fig. 7(a), the residual interaction pushes the levels apart, and the lower state crosses zero energy. However, the width Γ_- of this state, dashed lines in Figs. 7(b) and 7(c), is still positive. That would contradict energy conservation. For calculations shown by solid lines in Figs. 7(b) and 7(c) we account for the squeezing of the available phase space volume that forces the decay amplitudes to vanish once there is not enough energy for the process to take place. Similar to Ref. [33], we assume in the low energy region the square root energy dependence for the s -waves, and $\sim E^{3/2}$ for the p -wave,

$$\gamma_2(E) = \alpha\sqrt{E}, \quad \gamma_1(E) = \beta E^{3/2}. \quad (44)$$

Then the evolution of complex energies as a function of the strength v of the residual interaction is consistent with the existence of thresholds; at $v^2 = \epsilon_1\epsilon_2$ the lower state becomes stationary, $E_- = \Gamma_- = 0$. The near-threshold behavior of the width is governed by the s -wave component with the infinite slope, $\Gamma \sim \sqrt{E - E_-}$. However, as α becomes smaller, Fig. 7(c), the singularity is getting confined to a smaller vicinity of threshold, to the limit that at an observable scale the behavior is dominated by the p -wave.

Besides the trivial situation, when the width of a particular state vanishes due to energy conservation, blocking of the decay via dynamical mixing at a single point corresponding to some strength v is possible. This effect of the bound state in the continuum is seen in Fig. 7(b), where a conspiracy of the parameters leads to the vanishing width Γ_- of the lower state at energy E_- still in the continuum, Fig. 7(a). Eqs. (31a) and (31b) with $\Gamma_- = 0$ show that this happens at the interaction strength

$$v = A_1A_2 \frac{\epsilon_1 - \epsilon_2}{\gamma_1 - \gamma_2}. \quad (45)$$

Here $A_{1,2}$ and $\gamma_{1,2} = A_{1,2}^2$ are to be taken at the energy E_- found from Eq. (31a). For the model in Fig. 7(b) this happens at $v \approx 63$ keV. A similar case appears in Fig. 8 at $v \sim 185$ keV, where both states of the system become stable only at this particular mixing strength.

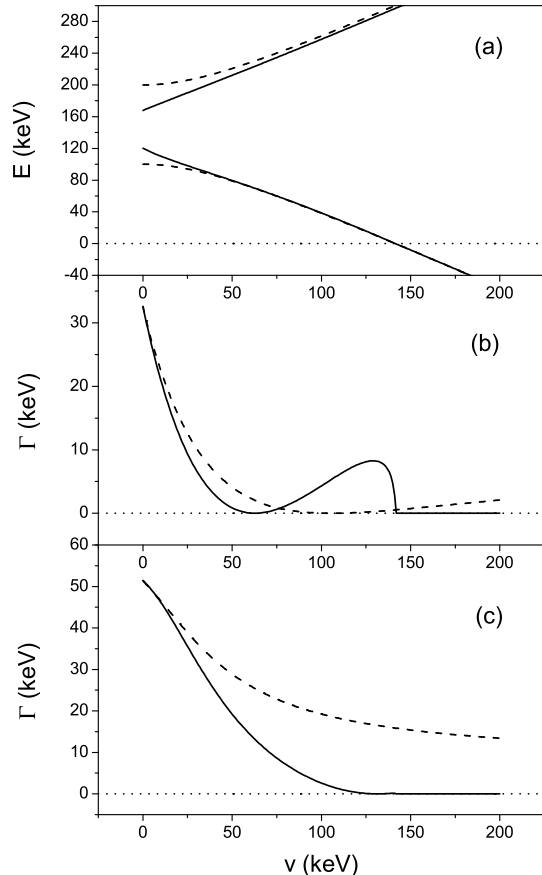


FIG. 7: Panels (b) and (c) demonstrate the behavior of Γ_- as a function of ν for energy-dependent (solid lines) and energy-independent (dashed lines) decay amplitudes. Selected parameters are: $A_1 = 8.1 (\text{keV})^{1/2}$ and $A_2 = 12.8 (\text{keV})^{1/2}$ in the energy-independent case, and $\alpha = 15 (\text{keV})^{1/2}$ and $\beta = 0.05 (\text{keV})^{-1/2}$ in the energy-dependent case, panel (b); $A_1 = 7.1 (\text{keV})^{1/2}$ and $A_2 = 3.1 (\text{keV})^{1/2}$, dashed line, and $\alpha = 1 (\text{keV})^{1/2}$ and $\beta = 0.05 (\text{keV})^{-1/2}$, panel (c). Parameters are selected in such a way that at $\nu = 0$ the two solid and dashed lines agree. The relative phases are such that $\nu \geq 0$ and $A_1 A_2 > 0$. In panel (a) energies of the two states are shown, solid lines, for the case relevant to panel (b) with the energy-dependent amplitudes, Eq. (44), and compared to the energies of a non-decaying system, dashed lines. The dotted line in all three plots corresponds to the zero value of the width or energy.

The energy dependence of the amplitudes complicates the motion of eigenvalues in the complex plane. Interesting features of the level crossing are demonstrated in Figs. 8 and 9. It should be emphasized that, unlike in a stable system or a system with energy-independent parameters, here the solutions for \mathcal{E}_+ and \mathcal{E}_- involve a diagonalization of different matrices. The Hamiltonian matrices differ in their imaginary part W . The “interaction” between lev-

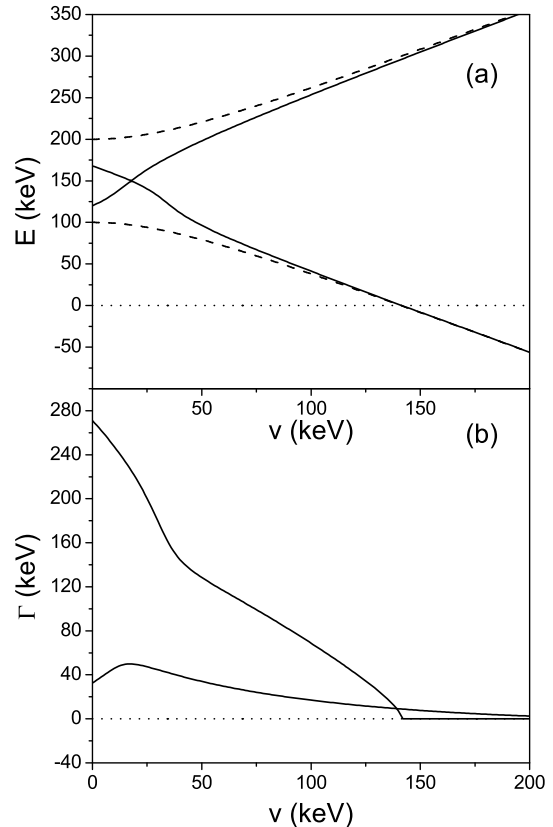


FIG. 8: Possible level crossing in a decaying system. Panels (a) and (b) show the energies and widths, respectively, for the two-level model of ^{11}Li . The upper panel, dashed lines, shows also the level repulsion in a closed system. The parameters used are the same as in Fig. 7(b), except for the opposite phase, $A_1 A_2 < 0$, for $\nu \geq 0$.

els occurs via common Hermitian part $H^\circ + V$. Thus for a general system it can be expected that bound and weakly bound states are still strongly correlated although some new features related to small imaginary components appear, and the usual level repulsion is present only up to a spacing of the order of the level width [13]. For states deeply in the continuum, however, the correlation must rely on the structure of $W(E)$, that represents features and symmetries of the continuum.

Figures 8 and 9 also emphasize the importance of relative phases for the matrix elements of the internal interaction and interaction to the continuum. We can always assume $\nu > 0$ as was done for our figures but the change in sign of $A_1 A_2$ leads to a system with very different properties, compare Figs. 7(a) and (b) to Fig. 8.

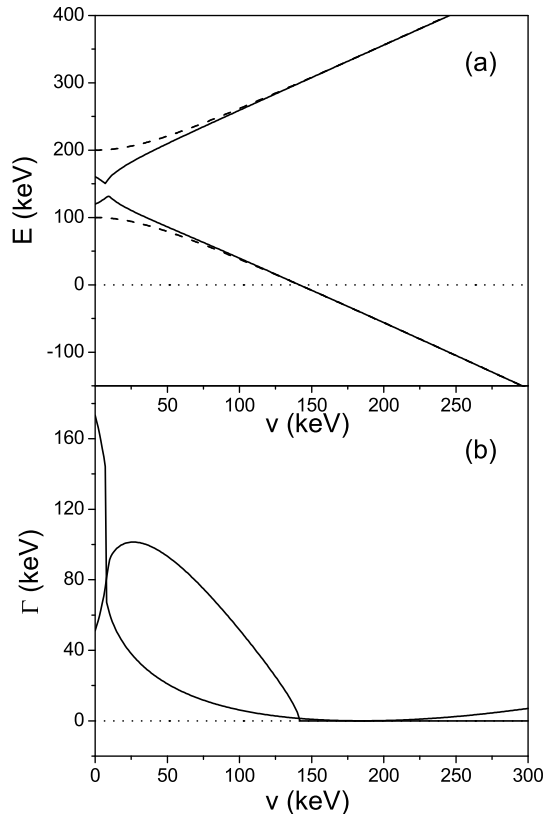


FIG. 9: Avoided crossing in a decaying system. See description for Fig. 8. Couplings are modified to $\alpha = 10(\text{keV})^{1/2}$ and $\beta = 0.05 (\text{keV})^{-1/2}$.

D. Cross sections near threshold

At the critical value of v , Eq. (25), and in the low energy region where the approximation (44) can be valid, the scattering amplitude (41) is singular, $\sim E^{-1/2}$,

$$T(E) \approx \frac{\alpha\epsilon_1}{\sqrt{E}\{\epsilon_1 + \epsilon_2 - (i/2)\alpha[\epsilon_2/(\epsilon_1 + \epsilon_2)]\sqrt{E}\}}. \quad (46)$$

When the interaction is over-critical, $v^2 > \epsilon_1\epsilon_2$, and at low energies, $E \leq |E_-|$ [Eq. (32)], we obtain

$$T(E) \approx \frac{\alpha\epsilon_1\sqrt{E}}{\mathcal{E}_+(E - E_-)}. \quad (47)$$

Therefore the cross section (40) has a constant value at threshold and behaves at low energies as $(E + |E_-|)^{-2}$ revealing “attraction” to the sub-threshold region [15]. Similar near-threshold resonance phenomena were discussed by Persson *et al.* [49]. The cross sections shown in Fig. 10(a) for two over-critical values of the interaction strength reveal a threshold behavior characteristic for loosely bound systems that can be mistaken for resonances. In this case we had $A_1A_2 > 0$ that produces

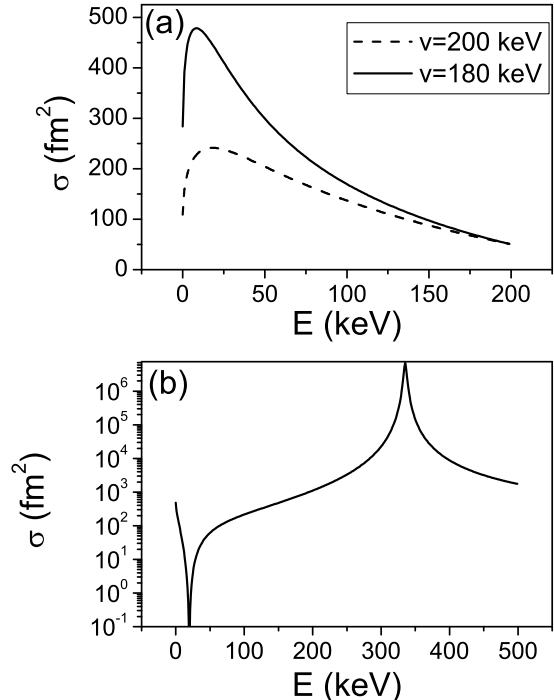


FIG. 10: The near-threshold scattering cross section is shown for loosely bound systems with $v = 180$ and 200 keV in solid and dashed lines, respectively. Due to similarity between the curves, the dashed curve is not shown in panel (b). Other selected parameters are $\alpha = 15 (\text{keV})^{1/2}$ and $\beta = 0.05 (\text{keV})^{-1/2}$. Phases are $A_1A_2 > 0$ and $A_1A_2 < 0$ for panels (a) and (b), respectively.

only a very broad peak (not shown on Fig. 10(a)) corresponding to the upper quasistationary state E_+ . The next Fig. 10(b) shows that in the case of $A_1A_2 < 0$ the interference of the internal and external interactions results in a narrow resonance with a very high cross section at $E = E_+ = 340$ keV, along with the maximum at zero energy (of course, all numerical values characterize only the model parameters).

VI. PAIRING IN THE CONTINUUM

In this Section we present examples of more realistic shell model calculations, where, in general, a large number of states is involved and further complications arise from the conservation of exact quantum numbers in the decay as well as from the required self-consistency between binding energies and thresholds for one and few-body decay channels.

The effective Hamiltonian \mathcal{H} implicitly depends on energy and other quantum numbers that determine if the decay is allowed by the conservation laws and what is the

near-threshold decay rate. Below we consider examples where the intrinsic configuration mixing is generated by the pairing interaction only. This leads to the conservation of all partial seniorities (a number of unpaired particles s_j on each orbital j). We will also use $s = \sum_j s_j$ as total seniority.

A. Two-level model

We again start with a simple model of a two-level system. We assume here that each level can accommodate $\Omega_1 = \Omega_2 = 10$ particles and both levels can decay to a final state that has fixed $E_f = 0$, their decay widths γ_1 and γ_2 are different but have the same, $\gamma_{1,2}(E) = \alpha_{1,2}\sqrt{E}$, energy dependence near threshold. It should be noted that introduction of a synchronous decay with $\gamma_1 = \gamma_2$ does not effect the internal dynamics since W in that case is proportional to a unit matrix. The corresponding single-particle energies are taken as $\epsilon_1 = 1$ and $\epsilon_2 = 3$. Intrinsic dynamics in this model are generated by the constant pairing $V_{L=0}^{jj'} \equiv G$. In Fig. 11 the spectrum of states with seniority $s = 0$ in the system of 8 particles is shown as a function of the pairing strength. The attractive pairing interaction pushes down low-lying levels, forcing some of them to become bound. The ground state becomes bound at $G \approx 0.2$.

Comparison of spectra with and without continuum coupling (solid and dashed lines, respectively) shows generic features. The bound states are not affected by the continuum coupling. The low-lying levels, as compared to highly excited states, are less influenced by the presence of continuum. In contrast to usual perturbation theory, we see that the ground state and even the first excited state once embedded in the continuum become attracted to the bulk of other states that increases their energy. Such a situation usually leads to an increase of the decay Q -value that in turn further increases the decay width.

The following Fig. 12(a) demonstrates the shift ΔE of the ground state energy as a result of decay for various choices of continuum coupling given by parameters α_1 and α_2 . Clearly, $\Delta E = 0$ if there is no configuration mixing at $G = 0$, or once the state becomes bound. The complex behavior of the decay width for the ground state is shown in Fig. 12(b); at the critical strength the width goes to zero with an infinite slope, $\sim \sqrt{E}$.

B. Realistic pairing model

As a demonstration of a realistic shell-model calculation we consider oxygen isotopes in the mass region $A = 16$ to 28. In this study we use a universal sd -shell model description with the semi-empirical effective interaction (USD) [50]. The model space includes three single-particle orbitals $1s_{1/2}$, $0d_{5/2}$ and $0d_{3/2}$ with corresponding single-particle energies -3.16354 , -3.94780 and

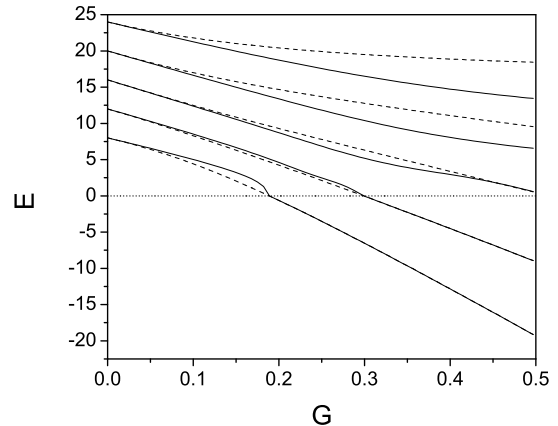


FIG. 11: The level scheme of $s = 0$ states in the two-level, 8-particle system as a function of pairing strength. Solid lines correspond to the system embedded in the continuum with the fixed width values $\alpha_1 = 0.1$ and $\alpha_2 = 5$. These curves are compared with a non-decaying situation $\alpha_1 = \alpha_2 = 0$ of the usual shell-model, dashed lines. The dotted line at $E = 0$ indicates the threshold location.

1.64658 MeV. The residual interaction is defined in the most general form with the aid of a set of 63 reduced two-body matrix elements in pair channels with angular momentum L and isospin t , $\langle (j_3\tau_3, j_4\tau_4)Lt | V | (j_1\tau_1, j_2\tau_2)Lt \rangle$, that scale with nuclear mass as $(A/18)^{-0.3}$.

Although the full shell model treatment is possible for such light systems, here we truncate the shell-model space to include only seniority $s = 0$ and $s = 1$ states. This method, “exact pairing + monopole”, is known [51] to work well for shell model systems involving only one type of nucleons (in the case of the oxygen isotope chain only neutrons are involved). The two important ingredients of nuclear forces are treated exactly by this method: the monopole interaction that governs the binding energy behavior throughout the mass region, and pairing that is responsible for the emergence of the pair condensate, renormalization of single-particle properties and collective pair vibrations. In our exploratory study, the truncation of the large space to the most important states is a reasonable approach since certainly the inclusion of decay makes the computations more numerically intense.

In the resulting shell-model description the set of the original 30 two-body matrix elements in the isospin $t = 1$ channel is reduced to 12 most important linear combinations. Six of these are the two-body matrix elements for pair scattering in the $L = 0$ channel describing pairing, and the other six correspond to the monopole force in the particle-hole channel,

$$\bar{V}_{j,j'} \equiv \sum_{L \neq 0} (2L + 1) \langle (j, j')L1 | V | (j, j')L1 \rangle, \quad (48)$$

where j and j' refer to one of the three single-particle

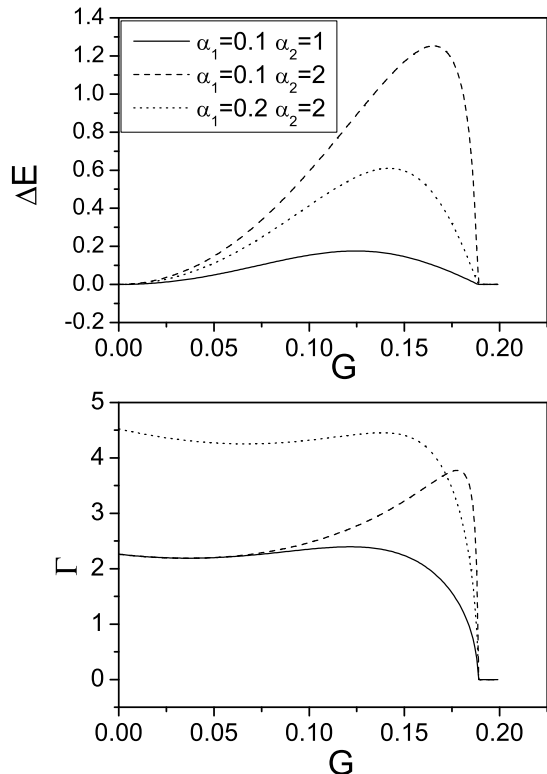


FIG. 12: The upper panel shows the shift in ground state energy between decaying and non-decaying (usual shell-model) systems, $\Delta E = E(\Psi) - E(\Psi_{s.m.})$, as a function of pairing strength under various assumptions for the decay rates. In the lower panel the width of the ground state is plotted.

levels.

We assume here that the orbital $0d_{3/2}$ belongs to the continuum and therefore its energy has an imaginary part. In this model we account for two possible decay channels for each initial state $|\Phi\rangle$, a one-body channel, $c = 1$, and a two-body channel, $c = 2$. The one-body decay changes the seniority of the $0d_{3/2}$ orbital by one, from 1 to 0 in the decay of an odd- A nucleus and from 0 to 1 for an even- A nucleus. The two-body decay removes two paired particles and thus does not change the seniority. The two channels lead to the lowest energy state of allowed seniority in the daughter nucleus, i.e. the possibility of transition to excited pair-vibrational states is ignored. This results in

$$e_{3/2}(\Phi) = \epsilon_{3/2} - \frac{i}{2}\alpha_{3/2}(E_{\Phi} - E^{(1)})^{5/2} - i\alpha_{3/2}(E_{\Phi} - E^{(2)})^{5/2}, \quad (49)$$

where we assumed that one and two-body decay parameters $\gamma_j^{(c)}$ are related as $\gamma_{3/2}^{(1)} = \gamma_{3/2}^{(2)}/2 \equiv \gamma_{3/2}$, and the

particles are emitted in the d -wave with $\ell = 2$.

These assumptions can be reviewed by examination of ^{17}O , where all three states with a valence particle located at one of the single-particle orbitals can be clearly identified as the $5/2^+$ ground state and $1/2^+$ and $3/2^+$ excited states. Their energies relative to ^{16}O exactly correspond to the single-particle energies in the USD model. Furthermore, experimental evidence indicates that the $3/2^+$ state decays via neutron emission with the width $\Gamma(^{17}\text{O}) = 96$ keV. This information allows us to determine our parameter $\alpha_{3/2} = \Gamma(^{17}\text{O})/(\epsilon_{3/2})^{5/2} = 0.028$ (MeV) $^{-3/2}$. Other two states are particle-bound, $\gamma_{1/2} = \gamma_{5/2} = 0$.

Using the complex single-particle energies, the effective non-Hermitian Hamiltonian for the many-body system is constructed in a regular way. We treat the chain of isotopes one by one starting from ^{16}O . Therefore for each A the properties of the possible daughter systems $A - 1$ and $A - 2$ are known. Since the effective Hamiltonian depends on energy, and all threshold energies have to be determined self-consistently, we solve this extremely non-linear problem iteratively. We start from the shell-model energies $E_{s.m.}$ corresponding to a non-decaying system with the Hamiltonian H . Then the diagonalization of $\mathcal{H}(E_{s.m.})$ allows us to determine the next approximation to the energies. This cycle is repeated until convergence that is usually achieved in less than ten iterations.

The results of the calculations and comparison with known experimental data for the chain of oxygen isotopes are shown in Table I. Despite numerous oversimplifications related to seniority truncation (some widths in the Table vanish only due to the fact that only $s = 0$ and $s = 1$ states were included), limitations on the configuration mixing and restrictions on possible decay channels and final states, the overall agreement observed in Table I is quite good. The results where experimental data are not available can be considered as predictions. In our view, however, the main merit of this calculation is in demonstrating the power of the method.

VII. CONCLUSIONS

The goal of the present paper is to demonstrate a variety of results that can be obtained with the use of an effective non-Hermitian Hamiltonian incorporated into the standard framework of the nuclear shell model. Although those ideas are known for a long time, right now it seems to be an appropriate moment to revive them and convert into a working tool for the solution of numerous practical problems of nuclear, and supposedly more general many-body, theory. In all cases when a many-body quantum system of strongly interacting particles is loosely bound, the interplay of the continuum and intrinsic structure is getting crucial, and the phenomena on the borderline between the bound states and reaction channels become exceedingly important. Therefore the formalism that would allow for a unified description of interrelated structure

A	J	E (MeV)	Γ (keV)	$E_{\text{exp.}}$ (MeV)	$\Gamma_{\text{exp.}}$ (keV)
16	0	0.00	0	0.00	0
17	5/2	-3.94	0	-4.14	0
17	1/2	0.78	0	0.87	0
17	3/2	5.59	96	5.08	96
18	0	-12.17	0	-12.19	0
19	5/2	-15.75	0	-16.14	0
19	1/2	1.33	0	1.47	0
19	3/2	5.22	101	6.12	110
20	0	-23.41	0	-23.75	0
21	5/2	-26.67	0	-27.55	0
21	1/2	1.38	0		
21	3/2	4.60	63		
22	0	-33.94	0	-34.40	0
23	1/2	-35.78	0	-37.15	0
23	5/2	2.12	0		
23	3/2	2.57	13		
24	0	-40.54	0	-40.85	0
25	3/2	-39.82	14		
25	1/2	2.37	0		
25	5/2	4.98	0		
26	0	-42.04	0		
27	3/2	-40.29	339		
27	1/2	3.42	59		
27	5/2	6.45	223		
28	0	-41.26	121		

TABLE I: Seniority $s = 0$ and 1 states in oxygen isotopes. Energies and neutron decay widths are shown. Results are compared to the known data. Ground state energies relative to the ^{16}O core are given in bold. The rest of the energies are excitation energies in a given nucleus.

and reaction aspects is especially needed, and many attempts in this direction made during recent years clearly demonstrate this need.

We illustrated the richness and nontrivial character of physics revealed by the complicated interplay of internal and external dynamics using a hierarchy of examples, from the simplest ones to less obvious to realistic many-body problems. Among the most interesting phenomena emerging here we can mention the redistribution of the widths, similar to the Dicke superradiance in optics,

and the segregation of direct processes from those going through the compound nucleus stage; interference of the “normal” intrinsic residual interaction and the interaction mediated by the excursion into open decay channels; dynamics of the poles in the complex energy plane with unusual crossings and anticrossings; emergence of bound states from the continuum; typical behavior of the reaction cross sections in the presence of loosely bound states. The correct account for the threshold singularities of the amplitudes of the processes at low energies was an indispensable part of the entire formalism. Finally, we have shown how realistic problems of nuclear structure can be solved with the aid of this method. In particular, the hybrid of the exact solution for the pairing interaction with the interaction through the continuum seems to be a promising instrument for future development of theory.

Certainly, the practical implementation of the method may be more complicated than in the standard shell model with bound states only. The self-consistency problems of two types, namely (i) a regular solution for the complex energies of quasistationary states governed by the energy-dependent Hamiltonian and (ii) the consistent determination of bound state energies, open channels and reaction thresholds for a chain of nuclides connected by those channels, may require new computational efforts.

The main theoretical problem that was not discussed above is related to the residual interaction necessary for the very formulation of the shell model problem in the presence of the continuum. In principle, the effective interaction should be energy-dependent and complex; it has to be consistent with the rest of the shell model input, including the amplitudes of the coupling to closed and open channels. This is a serious challenge for the future that requires a new insight into the whole physics on the borderline between structure and reactions.

Acknowledgments

The authors would like to acknowledge support from the NSF, grant PHY-0070911, and from the U. S. Department of Energy, Nuclear Physics Division, under contract No. W-31-109-ENG-38. V.Z. is thankful to the participants of the Workshop on Continuum Aspects of the Nuclear Shell Model (Trento, June 2002), where a part of this work was presented, for interest and discussions, and to the ECT* for hospitality and support.

-
- [1] V. Weisskopf and E. Wigner, *Z. Phys.* **63**, 54 (1930); **65**, 18 (1930).
[2] O. Rice, *J. Chem. Phys.* **1**, 375 (1933).
[3] U. Fano, *Nuovo Cim.* **12**, 156 (1935); *Phys. Rev.* **124**, 1866 (1961).
[4] H. Feshbach, *Ann. Phys.* **5**, 357 (1958); **19**, 287 (1962).
[5] C. Mahaux and H. Weidenmüller, *Shell-model approach*

to nuclear reactions (North-Holland Pub. Co., Amsterdam, London, 1969).

- [6] H. Barz, I. Rotter, and J. Hohn, *Nucl. Phys.* **A275**, 111 (1977).
[7] I. Rotter, *Rep. Prog. Phys.* **54**, 635 (1991).
[8] K. Bennaceur, F. Nowacki, J. Okolowicz, and M. Płoszajczak, *Nucl. Phys.* **A651**, 289 (1999); **A671**, 203 (2000).

- [9] N. Michel, W. Nazarewicz, M. Poszajczak, and K. Benaceur, Phys. Rev. Lett. **89**, 042502 (2002).
- [10] R. I. Betan, R. J. Liotta, N. Sandulescu, and T. Vertse, Phys. Rev. Lett. **89**, 042501 (2002).
- [11] J. Verbaarschot, H. Weidenmüller, and M. Zirnbauer, Phys. Rep. **129**, 367 (1985).
- [12] C. Lewenkopf and H. Weidenmüller, Ann. Phys. **212**, 53 (1991).
- [13] V. Sokolov and V. Zelevinsky, Phys. Lett. B **202**, 10 (1988); Nucl. Phys. **A504**, 562 (1989).
- [14] Y. Fyodorov and H.-J. Sommers, J. Math. Phys. **38**, 1918 (1997).
- [15] V. Sokolov and V. Zelevinsky, Ann. Phys. **216**, 323 (1992).
- [16] V. Sokolov and V. Zelevinsky, Fizika **22**, 303 (1990).
- [17] V. Sokolov, I. Rotter, D. Savin, and M. Müller, Phys. Rev. C **56**, 1031, 1044 (1997).
- [18] N. Auerbach, Phys. Rev. C **50**, 1606 (1994).
- [19] N. Auerbach and V. Zelevinsky, Phys. Rev. C **65**, 034601 (2002).
- [20] V. Flambaum, A. Gribakina, and G. Gribakin, Phys. Rev. A **54**, 2066 (1996).
- [21] A. Magunov, I. Rotter, and S. Strakhova, J Phys. B **32**, 1669 (1999); **34**, 29 (2001).
- [22] V. Pavlov-Verevkin, Phys. Rev. A **129**, 168 (1988).
- [23] M. Desouter-Lecomte and X. Chapuisat, Phys. Chem. Chem. Phys. **1**, 2635 (1999).
- [24] K. Pichugin, H. Schanz, and P. Šeba, Phys. Rev. E **64**, 056227 (2001).
- [25] P. Šeba, I. Rotter, M. Müller, F. Persson, and K. Pichugin, Phys. Rev. E **61**, 66 (2000).
- [26] R. Nazmitdinov, K. Pichugin, I. Rotter, and P. Šeba, Phys. Rev. E **64**, 056214 (2001); Phys. Rev. B **66**, 085322 (2002).
- [27] R. Dicke, Phys. Rev. **93**, 99 (1954).
- [28] P. von Brentano, Phys. Rep. **264**, 57 (1996).
- [29] V. Sokolov and P. von Brentano, Nucl. Phys. **A578**, 134 (1994).
- [30] M. Philipp, P. von Brentano, G. Pascovici, and A. Richter, Phys. Rev. E **62**, 1922 (2000).
- [31] E. Persson, I. Rotter, H.-J. Stöckmann, and M. Barth, Phys. Rev. Lett. **85**, 2478 (2000).
- [32] H.-J. Stöckmann, E. Persson, Y.-H. Kim, M. Barth, U. Kuhl, and I. Rotter, Phys. Rev. E **65**, 066211 (2002).
- [33] P. von Brentano, R. Jolos, and H. Weidenmüller, Phys. Lett. B **534**, 63 (2002).
- [34] V. Zelevinsky and A. Volya, in *Challenges of Nuclear Structure*, edited by A. Ciovoello (World Scientific, Singapore, 2002), p. 261.
- [35] I. Rotter, Phys. Rev. E **64**, 036213 (2001).
- [36] V. Sokolov and V. Zelevinsky, Phys. Rev. C **56**, 311 (1997).
- [37] V. Zelevinsky, in *RIKEN Symposium on Dynamics in Hot Nuclei* (RIKEN, 1998), p. 60.
- [38] P. Bortignon, A. Bracco, D. Brink, and R. Broglia, Phys. Rev. Lett. **67**, 3360 (1991).
- [39] S. Drozd, J. Okolowicz, M. Ploszajczak, and I. Rotter, Phys. Rev. C **62**, 024313 (2000).
- [40] A. Baz, I. Zeldovich, and A. Perelomov, *Scattering, reactions and decay in nonrelativistic quantum mechanics* (Nauka, Moscow, 1971).
- [41] F. Haake, F. Israilev, N. Lehmann, D. Saher, and H.-J. Sommers, Z. Phys. B **88**, 359 (1994).
- [42] E. Persson and I. Rotter, Phys. Rev. C **59**, 164 (1999).
- [43] P. Moldauer, Phys. Rev. C **11**, 426 (1975).
- [44] P. Kleinwachter and I. Rotter, Phys. Rev. C **32**, 1742 (1985).
- [45] P. Facchi and S. Pascazio, Phys. Rev. Lett. **89**, 080401 (2002).
- [46] M. Pfützner, E. Badura, C. Bingham, B. Blank, M. Chartier, H. Geissel, J. Giovinazzo, L. Grigorenko, R. Grzywacz, M. Hellström, et al., Eur. Phys. J. A **14**, 279 (2002).
- [47] H. Friedrich and D. Wintgen, Phys. Rev. A **32**, 3231 (1985).
- [48] P. von Brentano and M. Philipp, Phys. Lett. B **454**, 171 (1999).
- [49] E. Persson, M. Müller, and I. Rotter, Phys. Rev. C **53**, 3002 (1996).
- [50] B. Wildenthal, Prog. Part. Nucl. Phys. **11**, 5 (1984).
- [51] A. Volya, B. Brown, and V. Zelevinsky, Phys. Lett. B **509**, 37 (2001).